VIII International Conference on Particle-Based Methods
PARTICLES 2023
U. Perego, M. Cremonesi, A. Franci (Eds)

A COUPLED DEM-CFD MODEL TO STUDY THE PHYSICAL BEHAVIOR OF LOOSE ARMOR STONE REVETMENTS IN MARITIME WATERWAYS

J. SORGATZ[1], M. HERBST[2], H. KONIETZKY[2] AND M. POHL[1]

[1] Geotechnical Engineering in Coastal Areas
Federal Waterways Engineering and Research Institute (BAW)
Wedeler Landstraße 157, 22559 Hamburg, Germany
e-mail: julia.sorgatz@baw.de, webpage: https://www.baw.de

[2] Institute of Geotechnics
TU Bergakademie Freiberg
Gustav-Zeuner-Straße 1, 09599 Freiberg, Germany
e-mail: martin.herbst@ifgt.tu-freiberg.de, webpage: https://www.tubaf.org

Abstract. Revetments serve to protect a canal or river bank against erosion caused by natural and ship-induced waves and currents. A profound understanding of loads and resistances acting on revetments is indispensable for an economic and sustainable, but also safe revetment design. This paper presents a coupled CFD-DEM model (Computational Fluid Dynamics and Discrete Element Method) to study the physical behavior of loose armor stone revetments in maritime waterways. The waves and currents are modelled with a CFD add-on for the particle-based DEM software PFC3D. The DEM approach allows to simulate the shape, size and mass distribution and displacement of the individual armor stones realistically. DEM and CFD are coupled to capture the response of the armor stones to the hydraulic loads. In this paper, the model calibration and validation are presented using data derived from a full-scale flume experiment. The numerical model is compared to the flume tests where a slope is subjected to flow at different velocities. It can be shown that the implementation of revetment and hydraulic loads provides results that are consistent with the experimental data. Both flow velocities and armor stone displacements agree well between the physical and the numerical model. The herein presented study thus provides the basis for the application of the numerical model to more advanced stability analyses of revetments that are, e. g., subjected to wave and current attack.

Keywords: Discrete Element Method (DEM), Computational Fluid Dynamics (CFD), coupled simulation, revetment design, physical flume tests, wave and current attack.

1 INTRODUCTION

Revetments usually consist of an erosion-resistant cover layer, a filter layer and, in the case of artificial waterways that lie above the groundwater level, a sealing layer. The top layer can be constructed in different ways, e. g., loose, fully or partially grouted armor stones or technical biological constructions (see **Figure 1**). The herein presented work focuses on loose armor stone revetments in maritime waterways.

The present design principles for revetments, e. g., [1-4] are based on empirical values, physical model approaches and small-scale model tests that mainly cover either inland waterways or coastal protection structures. So far, the interaction of hydraulic loads and loose armor stone revetment in the estuary areas and maritime waterways that are particularly subjected to large tidal water level changes as well as waves and currents from passing seagoing vessels has been investigated little.

Figure 1: Typical bank protections in inland and coastal areas: technical-biological bank protection (left), loose armor stone revetment (center) and fully-grouted revetment (right)

When a ship is travelling through the water, wave systems of different periods occur due to the flow caused by the ship (Bernoulli current) and the pressure and water level changes that occur at the bow, stern and longitudinal side of the ship. The changes in water level in a depth- and side-limited fairway, as the wave system appears to an observer on the shore, are explained schematically in **Figure 2** (left). In their chronological sequence, the following changes in the water level at rest become clear: bow swell, drawdown as the difference between bow swell (or surge wave) and maximum water level drawdown, primary wave (as stern wave) as well as the secondary wave system overlapping the primary wave. The resulting ship-generated flow is shown in **Figure 2** (right). The magnitudes of water level fluctuations and currents generated by moving ships are particularly affected by the ship's speed and passing distance to the shore, the blockage ratio (relation of vessel size to cross-sectional area of fairway) and the relation of water depth to vessel draught. A detailed description of the different components of the ship-induced loads and the influencing factors can be found in [5].

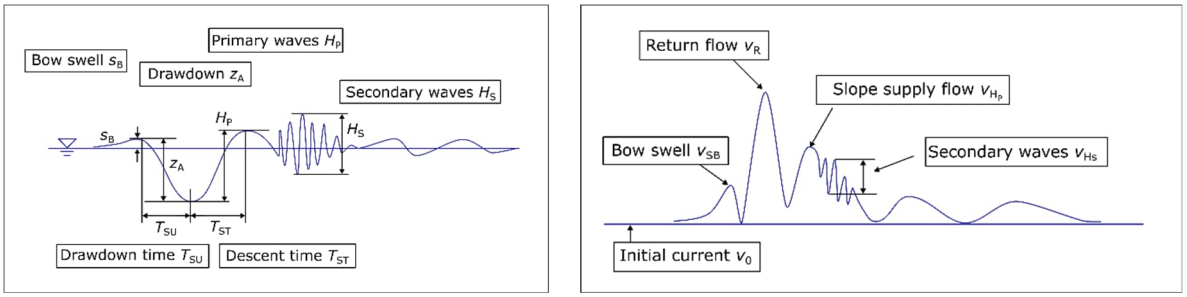

Figure 2: Schematic lateral view of the ship's wave systems (left) and resulting ship-generated flow (right)

Numerical methods can help to investigate and, eventually, to understand these interactions in more detail. The overall objective of the presented research is to develop a coupled CFD-

DEM (Computational Fluid Dynamics and Discrete Element Method) model that can be used to determine the resistances of loose armor stone revetments for the boundary conditions along maritime waterways and, thus, to supplement existing design procedures and codes. The required numerical model set-up is unique since it requires that large particles, i. e., armor stones, are subjected to a complex scheme of hydraulic loads, i. e., ship-induced waves and currents, which, in turn, is affected by the armor stones. This paper presents excerpts of the implemation, calibration and validation of the numerical model using a full-scale flume experiment. The presented study provides the basis for the use of the numerical model in more advanced stability analyses of revetments subjected to (ship-induced) waves and currents.

2 PHYSICAL FLUME TEST

2.1 Geometry and model set-up

The physical flume tests are designed to gather data for the calibration and the validation of the numerical model. For the experiments, the large hydraulic flume of the Federal Waterways Engineering and Research Institute in Hamburg was used. It works as a recirculating flume with a total length of 204 m, of which 80 m are designed as a straight rectangular flume with a cross-section of 1.47 m *x* 1.50 m. The maximum filling level is 1.30 m; the maximum flow velocity in the unobstructed cross-section amounts to $v \approx 1.5$ m/s. Higher flow velocities can be achieved in obstructed cross-sections. Two different slope inclinations of the revetment were investigated: a 1:1 (V:H) slope and a 1:3 (V:H) slope.

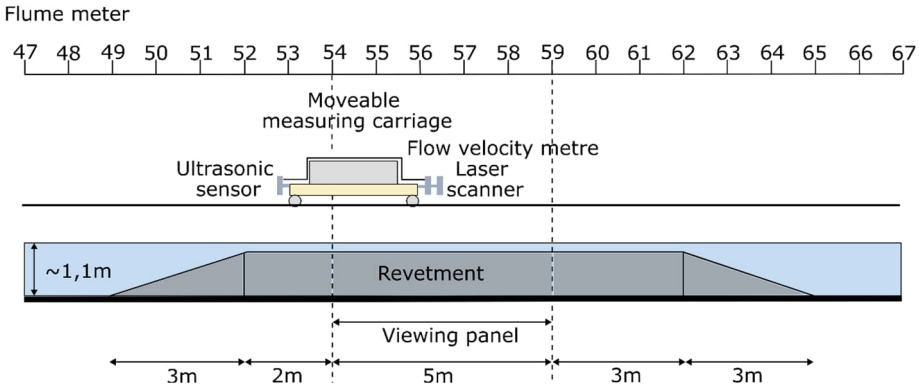

Figure 3: Geometry and measurement set-up of the physical flume tests

The armor stones used throughout the experiments are andesite stones from the Mammendorf quarry in Germany. The size of the armor stones corresponds to the armor stone class $CP_{90/250}$ [6] with a mean nominal diameter $D_{n,50}$ = 109 mm (σ = 27.92 mm) and a mean mass m = 2.69 kg (σ = 1.93 kg). The armor stone density ρ_s varies between 2300 kg/m³ and 2650 kg/m³. The friction angle of the armor stones $\phi_s = 45°$ and the void ratio of the revetment n = 0.45 were estimated conservatively according to common literature [1].

2.2 Measurment devices

A moveable measuring carriage (see **Figure 3**) was equipped with a bridge and adapters that

allowed to install different sensor units. The attached sensor system could be moved in the longitudinal direction of the flume (FM) via the carriage drive; positioning orthogonal to the flume axis (*x*-direction) and at different water levels (*y*-direction) was possible via a crossbeam. The control software allowed to record profiles at any longitudinal and orthogonal position.

Highly accurate acoustic 3D ADV flow sensors (Acoustic Doppler Velocimeter) were used to record the flow velocities. With these particular sensors, the flow velocity is derived from a shift in the transmission frequency. Moving particles of suspended matter within the measurement volume cause a reflection in the output signals. The sensors have an accuracy of 1 % (± 2.5 cm/s at maximum range). After the system has been parameterized with the current water temperature and salinity, no further calibration is necessary.

The armor stone displacements were documented by means of photos. For this purpose, the armor stones were colored in stripes of 0.50 m. Moreover, the surface geometry of the revetment was recorded with laser scans. Measurements were conducted in a grid of 5 mm x 5 mm with the moveable measuring carriage.

2.3 Test procedure and data analyses

A total of four campaigns (1:1 slope, 1:3 slope and a repetition of each) were studied. The experimental procedure followed the same scheme in each campaign: The flow velocity v was increased in four steps from approx. 1 m/s to 2 m/s. Immediately after each flow step and approx. 40 s of flow at the precribed flow velocity, the flow was stopped and the water discharged from the flume. Subsequently, the displacement of the armor stones was recorded. The revetment itself was not changed during one campaign.

In post processing, the total flow velocities were determined from the individual flow velocity components measured in *x*-, *y*- and *z*-direction. The height differences to evaluate the armor stone displacements were computed between the previous and the subsequent laser scan using the software Surfer (version 15). The photos were evaluated manually and used to validate the height difference plots obtained from the laser scans.

2.4 Experimental results

Figure 4 shows examplary the measured flow velocities over the flume metres (FM) for the 1:1 slope. The measurement locations are referenced by their horizontal and vertical distance to the left flume wall where the slope is supported, e. g., the measurement point “030-080” is located 30 cm (*x*-direction) from the wall and 80 cm (*y*-direction) above the flume bottom. It can be noted that the flow velocity increases continuously with increasing FM until the slope starts to fall again due to the cross-sectional constriction and the interaction of flow and armor stones. At high flow velocities (1.7 - 2.1 m/s), turbulent flow occurs, which, however, cannot be recorded with the sensors (missing points in **Figure 4**, right).

To illustrate the armor stone displacements, the height different plots from the 1:1 slope are shown in **Figure 5**. During the first flow step a few armor stones moved slightly, which can also be described as “initial settlement” of the revetment. However, no large-scale armor stone displacements took place. At $v = 1.40$ m/s, a single armor stone was displaced. Only at $v \approx 1.70$ m/s significant armor displacements were observed. In the case of the 1:3 slope, only few armor stones moved. If a displacement occured, it was a downward movement of a single armor stone towards the toe of the slope.

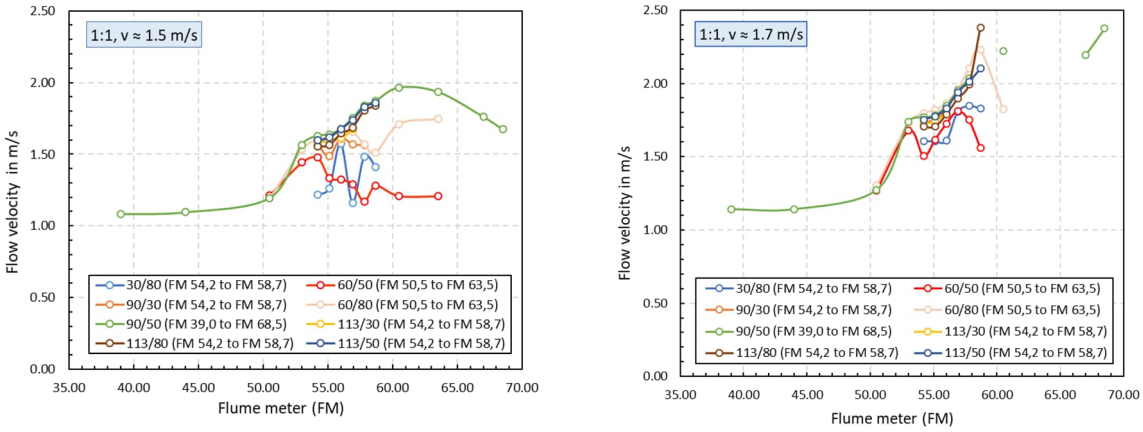

Figure 4: Flow velocities measured along the flume for the 1:1 slope

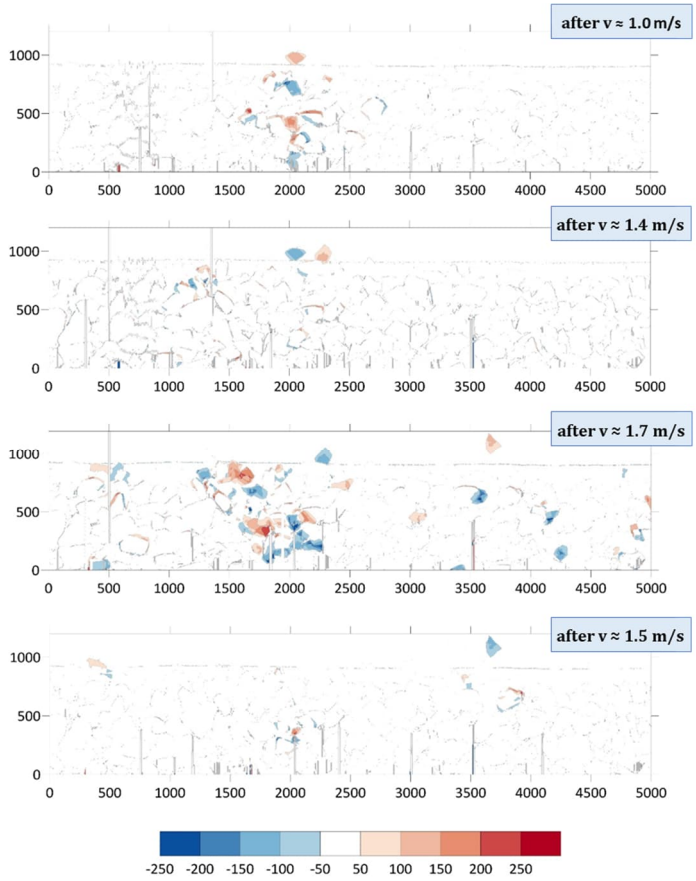

Figure 5: Height difference plots for visualization of the stone displacements (in mm) for the 1:1 slope. The blue coloring indicates erosion, the red coloring deposition, white-colored areas indicate no displacement.

In summary, the flume experiments indicate that for the armor stone size chosen in the experiments, armor stone displacements must be expected for $v > 1.7$ m/s. This observation corresponds to present design equations [1] that predict armor stone displacements from

$v \approx 1.7$ m/s onwards for the 1:1 slopes. For slopes with an inclination of 1:3, the armor stones start moving from $v \approx 2.0$ m/s onwards.

3 COUPLED DEM-CFD MODEL

3.1 DEM and PFC3D-CCFD add-on

The Discrete Element Method (DEM) is a numerical method for simulating the motions and interactions of particles of a discontinuous medium based on Newton's 2nd law and contact laws. The DEM method was originally developed by Cundall and Strack [8]. Today, it is widely used for investigations of various solid as well as granular materials. For our purpose, the DEM allows to model the armor stones as independent objects. It provides a realistic representation of their mechanical behavior with three translational and three rotational degrees of freedom.

In this particular project, the DEM-related part of the modelling is done by applying the three-dimensional code PFC3D [9] developed by the ITASCA CONSULTING GROUP INC. The use of spherical particles (balls) facilitates the contact detection. Only point contacts are possible and a contact between two objects only depends on their distance. Complex shape geometries can be realized by merging overlapping balls into so-called “clumps”.

The hydraulic impacts are modelled with a “Coupled Computational Fluid Dynamics” (CCFD) software that is available as an add-on in the PFC3D versions 5 and 6. The CCFD add-on requires Visual Studio (version 2011) for implementing user-defined boundary conditions and GID (version 8.0.9), a pre- and post-processor, in which the model construction and the flow evaluation take place. Simple boundary conditions are available in GID, more complex ones can be programmed in C++ using the Visual Studio software. Laminar and turbulent flow conditions, non-Newtonian and free-surface (two-phase) flow can be modelled in this way.

PFC3D uses a so-called “coarse-grid-scheme” to model the fluid flow. This aproach requires the CFD fluid cells to be significantly larger than the modelled PFC3D elements, i. e., the relatively large armor stone clumps. In order to enable flow calculation, a minimum porosity of 5 % must be ensured in each CFD cell. This has direct consequences on the modelling results as only integral effects of the fluid flow on the PFC3D elements located in a fluid cell can be captured by the model. Flow within the pore space of the revetment cannot be simulated.

Incompressible viscous fluid flow is assumed since the expected pressure gradients are small and the compressibility of the fluid is thus negligible. Then, the divergence of the fluid field is:

$$\nabla \cdot (\vec{v}) = 0 \tag{1}$$

with the fluid velocity vector $\vec{v}$. The Navier-Stokes equation can then be written as

$$\rho_f \left(\frac{\partial \vec{v}}{\partial t} + (\vec{v} \cdot \nabla)\vec{v}\right) = -\nabla p + \mu \nabla^2(\vec{v}) + \vec{f} \tag{2}$$

with the fluid density ρ_f, the time t, the fluid pressure p, the dynamic viscosity μ and the normalized volume force $\vec{f}$, i. e., gravity and coriolis force. Equation (2) is valid for flow without any particles. When accounting for the material, the porosity ϵ is smaller than 1 and the equations (1) and (2) become

$$\frac{\partial \epsilon}{\partial t} + \nabla \cdot (\epsilon \vec{v}) = 0 \tag{3}$$

$$\rho_f \left(\frac{\partial \epsilon \vec{v}}{\partial t} + (\vec{v} \cdot \nabla)\epsilon \vec{v}\right) = -\epsilon \nabla p + \mu \nabla^2 (\epsilon \vec{v}) + \vec{f}. \quad (4)$$

Within the DEM sequence an additional fluid force term is included:

$$\frac{\partial \vec{u}}{\partial t} = \frac{\vec{f}_{mech} + \vec{f}_{fluid}}{m} + \vec{g} \quad (5)$$

where $\vec{u}$ is the velocity vector of the particles, $\vec{g}$ is the gravity vector, $\vec{f}_{mech}$ is the mechanical force, m is the particle mass and $\vec{f}_{fluid}$ is the fluid force applied to the particles containing the drag force, the pressure gradient and the buoyancy.

3.2 Fluid flow algorithm

There are many methods to solve the Navier-Stokes equations for fluid flow. The so called SIMPLE algorithm is used within the CCFD add-on. SIMPLE stands for **S**emi **I**mplicit **M**ethod for **P**ressure **L**inked **E**quations. This algorithm solves the problem iteratively for each fluid cell. Firstly, the boundary conditions are applied and evaluated at the cell boundaries. Secondly, the momentum equation for the resulting fluid velocity vector is solved. From this, the pressure gradient term can be calculated. Finally, the fluid velocity vector and pressure are adjusted iteratively until a volume conservative solution is found. This procedure is repeated for each fluid cell over the simulated model time.

To apply the method successfully, some common pitfalls have to be considered. Firstly, incompatible boundary conditions are not detected by the pre-processor. The user has the full reponsibility to ensure that the applied boundary conditions are accurate. Secondly, zero porosity may occur. If the porosity in a cell becomes less than 5 %, a warning by PFC3D is issued. In the case of zero porosity, the calculation stops with an error message. Reduced particle stiffness may also lead to problems because heavy particles overlap resulting in strong contact forces and accelerations. Numerical instability is possible, especially when many particles are removed or added instantaneously to a fluid cell within one time step.

3.3 Numerical flume models

As the numerical model should provide a realistic representation of the revetment with regard to the single armor stones as well as the stability of the cover layer, i. e., the interlocking effects of individual armor stones, the armor stones are assigned to different size and shape categories (platy, elongated, compact), whereby a mixed group with armor stones of all categories is used in the numerical models [10]. Furthermore, the particle shape can be designed in a high or low resolution depending on the number of balls used to form a clump. The more complex the geometry of the clumps, the better the representation of the interaction between the armor stones. However, the computation time increases exponentially with increasing clump complexity. The behavior of the clumps is also affected by the friction coefficient of the particle surface and, indirectly, by the stiffness of the particle contacts. Accordingly, particularly for armor stones of lower resolution, these parameters are to be calibrated in a way that approximates the behavior of the armor stones for armor stones in nature.

In the herein presented study, a ball packing with a moderate number of balls per clump is used. It is a rough approximation with regard to the armor stone geometry as a compromise between the time required for a simulation run and the model's accuracy. **Figure 6** shows the

generated clump templates used throughout all the simulations. The sizes of the numerical armor stones are scaled to match the mass distribution in nature. Moreover, since the armor stone density ρ_s varied between 2300 kg/m³ and 2650 kg/m³ in the flume experiments, models with ρ_s = 2300 kg/m³ and ρ_s = 2650 kg/m³ were investigated. **Figure 7** shows the cross-section of the numerical model with overlaying experimental measurement positions. The outer boundaries are represented by planar faces, so called walls.

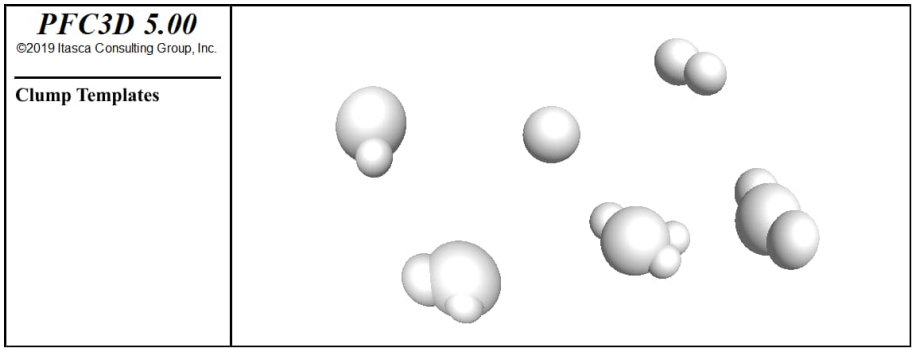

Figure 6: Clumps representing different armour stones

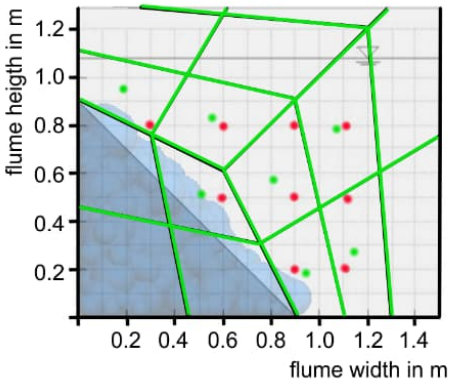

Figure 7: Flume-cross section with measurement locations in the experiment (red), PFC3D clumps (light blue) and CCFD fluid cells with center point (green) for the 1:1 slope (dark blue triangle)

4 RESULTS OF THE NUMERICAL ANALYSES

4.1 Calibration of the numerical model with the flume measurements

PFC3D offers several contact laws including user defined contact models. For this study, the standard linear contact model was chosen as it is well approved and capable of reproducing the contact behavior of a wide range of particle sizes starting from fine sand up to huge blocks. The linear contact model assumes spring forces and friction. It is characterized by the normal stiffness k_n, shear stiffness k_s, friction coefficient μ, normal damping ratio β_n and shear damping ratio β_n. Stiffness is given in force per length, friction coefficient and damping ratios are dimensionless.

The damping ratios allow to define the proportion of energy dissipation in the mechanical system. Without damping and friction the linear contact model simulates a perfect elastic particle collision. PFC3D allows to use different parameter sets for the armor stone to armor stone and the armor stone to wall contact. However, since the characteristics of the wall surface are similar to those of the armor stones, a common parameter set was chosen.

To obtain realistic results with respect to the flow velocities and armor stone displacements in the numerical model, a calibration procedure in the mechanical calculation part within PFC3D is required. Starting with an approximated set of values the parameter for the contact model are modified until flow velocities and armor stone displacements in the physical and numerical model tests are similar. The following values for the contact model were determined: friction coefficient μ = 5.5, stiffnesses $k_n = k_s$ = 1E8 N/m, damping ratios $\beta_n = \beta_s$ = 0.4. With these parameters the numerical models show the in the following section presented results.

4.2 Comparison of flow velocities in physical and numerical model

Figure 8 shows a comparison of the experimental measured velocities (dots) compared with the numerical values. In **Figure 9** the differences between the flow velocities in the physical flume tests and numerical simulations are given for three / four measurement locations in the flume. Once again, the measurement locations are referenced by their horizontal and vertical distance to the left flume wall (see Chapter 2.4). If measurement locations in the physical and the numerical model were not entirely the same, values of similar relative position to the revetment structure or mean values of two positions are chosen for comparison.

The comparison shows that the numerical model both overestimates (positive difference) and underestimates the flow velocities (negative difference). For the majority of locations, the numerical model overestimates the flow velocities. The difference increases with an increasing overflow distance (increasing FM). Only at the upper left edge of the model near the flume wall flow velocities are underestimated. For the models with larger armor stone density, the deviations are slightly smaller. Overall, however, the flow differences are within an acceptable range. The simulation with PFC3D and CCFD produces realistic flow velocities, although with significantly lower fluctuations than the physical tests, which is likely due to the “coarse grid scheme”. Essentially, only macroscopic flow effects on the armor stones are replicated.

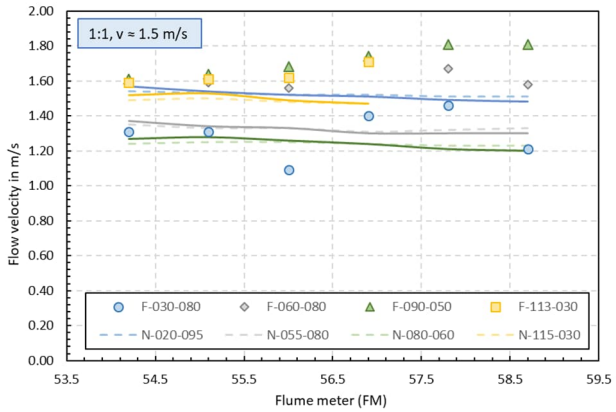

Figure 8: Comparison of the flume measurements (F) and the numerical flow velocities (N) for the 1:1 slope, v = 1.5 m/s, ρ_s = 2300 kg/m³ (dashed lines) and ρ_s = 2650 kg/m³ (solid lines)

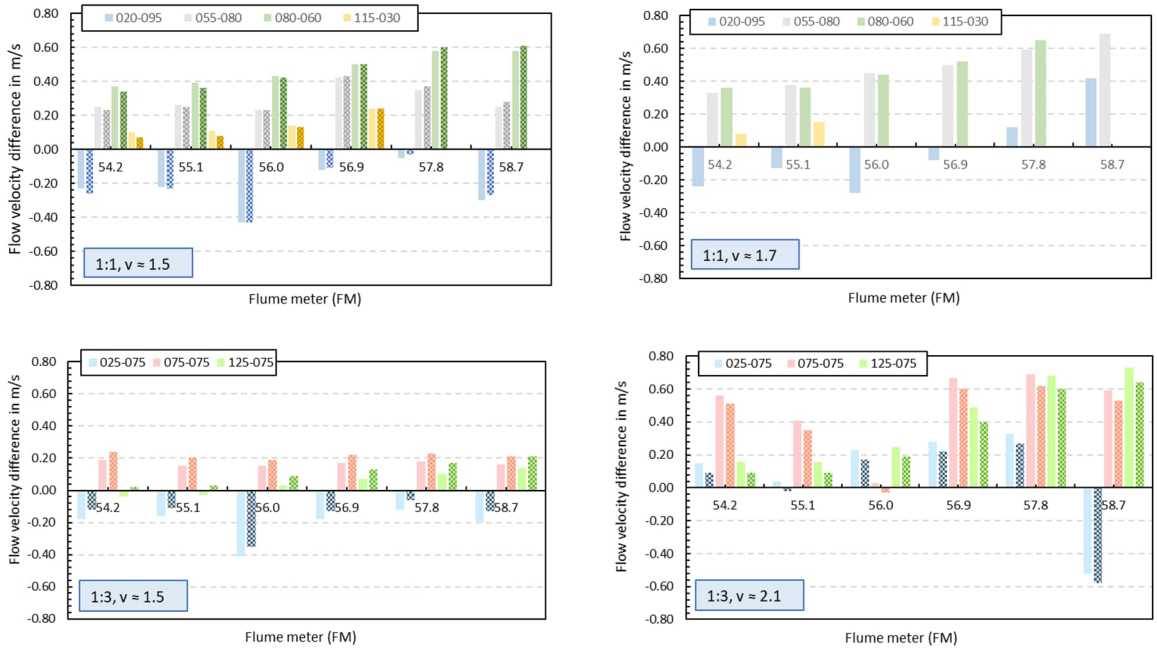

Figure 9: Flow velocity differences observed between physical model and numerical model tests; light shaded bars refer to investigations with ρ_s = 2300 kg/m³; dark shaded, hatched bars to ρ_s = 2650 kg/m³. Light and dark shaded bars were each measured at the same flume location.

4.3 Comparison of armor stone displacements in physical and numerical model

For a comparison of the armor stone displacements, vertical difference plots are available from the physical flume tests (see **Figure 6**). In PFC3D, the displacement components in the coordinate directions, the displacement magnitudes (each in m) and the absolute displacement vectors (in length units, scaled to a "favorable" size) are evaluated. As the displacements in the physical and the numerical model therefore do not represent the same values, the herein presented comparison focuses on a qualitative rather that a quantitative comparison.

In **Figure 10** (1:1 slope and v = 1.5 m/s) it can be noted that, contrary to the physical flume tests, only erosion occurs (blue). Most of the displacements are observed right at the start of the simulations. This may indicate the initial settlement of the structure, i. e., the armor stones move into more stable positions. Yet, installation effects, as they are present in the physical flume tests, cannot be inferred from the numerical simulations.

The results of the 1:1 and 1:3 slope in the numerical simulations are very similar and more similar to each other than those of the physical tests, which is probably caused by the "coarse grid scheme". Furthermore, in all numerical models, movements perpendicular to the direction of flow can be observed, i. e., the slope flattens. Very large displacements are mainly caused by the relatively round clumps that literally roll off to the flume bottom. Here, the influence of the simplified clump shape is clearly noted. In summary, however, over all variations considered, a good agreement of the observed armor stone displacements was found.

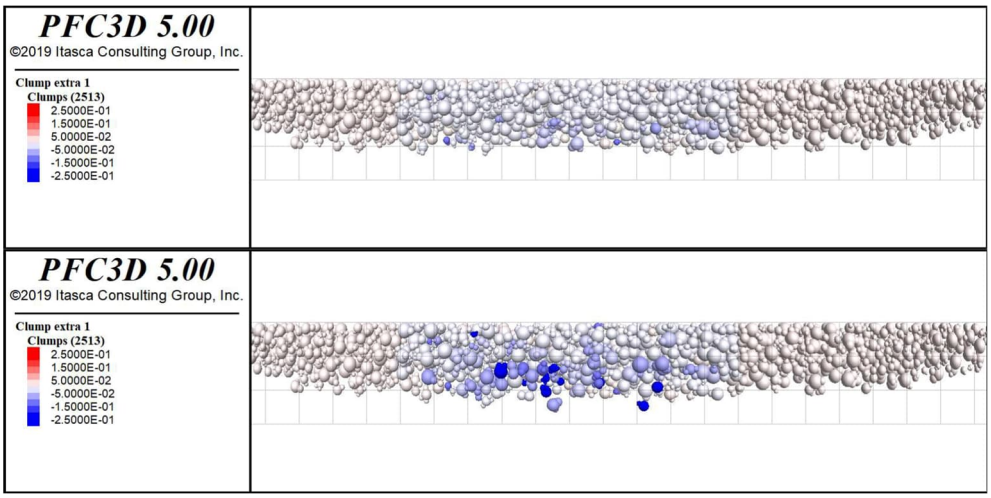

Figure 10: Difference plot of the armor stone displacements in m for 1:1 slope, v = 1.5 m/s and ρ_s = 2300 kg/m³; directly after the start of the simulation (top) and after 40 s of flow (bottom).

5 DISCUSSION

The investigations show that revetment models with constant flow boundary conditions and simple geometries can be implemented relatively well in PFC3D and CCFD. A good agreement between the flow velocities and the armor stone displacements in the numerical analyses and the physical experiments was found. A more detailed representation of the armor stone shapes may lead to more accurate results. Larger armor stone displacements due to rolling clumps at the flume bottom may be averted. Although, it is assumed that this effect is of less importance for the total revetment stability.

Based on the flow measurements in the physical model, it can be assumed that turbulent flow occurred in some areas. This phenomenon was particularly observed for the 1:3 slope, where the cross-section of the flume was blocked by the 1:3 slope. To what extent these turbulences may affect the measurements and also the armor stone displacements in the physical experiments cannot be inferred from the data. At the same time, however, a major drawback of the present numerical model becomes obvious. The interaction between the revetment and flow and, thus, resulting turbulences cannot be represented in the numerical model. Since the "coarse-grid-scheme" approach requires the CCFD fluid cells to be significantly larger than the PFC3D elements, only integral effects of the fluid flow on the PFC3D elements can be replicated.

Moreover, the meshing has a large influence on the success of a simulation. For example, the refinement of the mesh by an additional fluid cell layer (instead of n now n+1 element in any coordinate direction) can lead to the simulation stopping after one or a few iterations. A major problem at the beginning of the simulation is that, depending on the flow direction, strong system reactions can occur due to sudden large accelerations. This happens especially with low porosities (below approx. 20 %) and leads to numerical instabilities and system failures. A feasible solution is to first conduct the flow simulation without coupling and, in the second step, to introduce the thereby determined flow field in the PFC3D model. This procedure works as

the interaction between the PFC3D elements and the flow is small and essentially only affected by the porosity of the fluid cell.

In general, the PFC3D calculations are very time-consuming when using the CCFD add-on, since, in addition to the flow calculation, there are usually very small time-steps in the PFC3D (1E-7 ... 1E-5 s), so that a large number of iteration steps is necessary to solve a simulation.

6 CONCLUSIONS

This paper provides insights into the calibration and validation of a coupled CFD-DEM model using full-scale flume tests. The model characteristics, initial and boundary conditions are chosen in a way that, eventually, the model will be able to replicate the stability of bank protections in estuaries subjected to ship-induced waves and currents.

The investigations show that revetment models with constant flow boundary conditions and simple geometries can be implemented relatively well with PFC3D and CCFD. The results of the flume can be reproduced numerically. At the same time, some deficits of the CCFD-PFC3D models became apparent. For instance, as a result of the “coarse-grid-scheme” the numerical results are mainly qualitative in nature.

Future work should continue the development of the numerical model to allow modelling a real interaction of flow and armor stones as well as turbulences. Moreover, the complex combination of ship-induced waves and currents (see **Figure 2**) must be implemented.

REFERENCES

[1] Bundesanstalt für Wasserbau (ed.), *BAW Code of Practice Principles for the Design of Bank and Bottom Protection for Inland Waterways (GBB)* (2010).

[2] Hansen, U. A., *Wasserbausteine im Deckwerksbau, Bemessung und Konstruktion* [Armor stone in revetment construction, design and construction]. Heide: Westholsteinische Verlagsanstalt Boysens & Co (1985).

[3] KFKI (ed.), “Empfehlungen für die Ausführung von Küstenschutzwerken (EAK)” [Recommendations for the execution of coastal protection works]. *Die Küste*, **65** (2007).

[4] CIRIA; CUR; CETMEF, *The Rock Manual. The use of rock in hydraulic engineering*, 2. ed. London (2007).

[5] Schneekluth, H., Hydromechanik zum Schiffsentwurf [Hydromechanics for ship design]. 3. Auflage, Herford: Koehlers Verlagsgesellschaft (1988).

[6] Technische Lieferbedingungen für Wasserbausteine (TLW). (2022).

[7] Bundesanstalt für Wasserbau, Elbinsel Lühesand – Geotechnischer Bericht zur Bemessung der Ufersicherung [Elbe island Lühesand - Geotechnical report on the design of bank protection] (BAW-Gutachten, A39550110266) (2017).

[8] Cundall, P. A.; Strack, O. D. L., A discrete numerical model for granular assemblies. In: Géotechnique, 29 (1), S. 47-65, https://doi.org/10.1680/geot.1979.29.1.47 (1979).

[9] Itasca Consulting Group Inc., PFC3D3D. Particle Flow Code in 3 Dimensions. User‘s Manual. Version 4.0. Minneapolis (2008).

[10] Mittelbach, L.; Pohl, M.; Schulze, P.; Konietzky, H., Numerical Simulation of Rip-Rap Revetments in Tidal Areas, Die Küste, 81, p. 119-132 (2014).